Enhancing VR Mandala Drawing and Natural Immersion for Attention Restoration with AI-Driven Bioadaptive Multimodal Interaction

Tiantian Geng
The University of Aizu,
Aizu-Wakamatsu, Japan
Aizuwakamatsu, Japan
ttgengw@gmail.com

Huishan Lai
The University of Aizu,
Aizu-Wakamatsu, Japan
Aizuwakamatsu, Japan
huiishan99@gmail.com

Lei Jing
The University of Aizu,
Aizu-Wakamatsu, Japan
Aizuwakamatsu, Japan
leijing@u-aizu.ac.jp

Abstract

Digital attention fatigue is a pervasive challenge, yet restorative virtual reality still lacks clear guidance on how interaction design and in-process adaptation can support attention regulation goals. Grounded in Attention Restoration Theory and an attentional-ecology perspective, we present a system that *enhances virtual reality mandala drawing and natural immersion* with *AI-driven bioadaptive multimodal interaction*. The experience integrates structured mandala drawing within a static 360° nature scene; using real-time heart rate variability, the adaptive loop modulates visual haze, ambient audio, and synchronized haptics through lightweight machine-learning-based state estimation and online gain personalization. In a within-subject pilot study, we compared a *no-multimodal-feedback condition* with an *AI-driven bioadaptive multimodal interaction condition* that added bioadaptive multimodal feedback to the same VR nature-and-mandala experience. Outcomes were evaluated using self-report measures of presence and perceived restorativeness, behavioral measures, autonomic measures, and electroencephalography measures. While both conditions were experienced as generally restorative, adding bioadaptive multimodal interaction dampened arousal-related Cz β activity relative to the no-multimodal-feedback condition and showed consistent trends toward higher presence. Exploratory analyses further suggested a condition-specific coupling in which PRS Fascination covaried with reaction-time improvement only when bioadaptive multimodal interaction was enabled. Together, the results provide initial evidence that psychology-theory-guided experience design paired with a personalized bioadaptive interaction mechanism can shape regulatory outcomes, and that multidimensional evaluation can disentangle perceived restoration from measurable behavioral and neurophysiological regulation.

CCS Concepts

• **Human-centered computing**; • **Computing methodologies**; • **Applied computing**;

Keywords

Human Augmentation, Attention Restoration Theory (ART), Virtual Reality (VR), Artificial Intelligence (AI), Attention Restoration, Mandala Drawing, Multimodal Feedback, Bioadaptive Interaction

ACM Reference Format:

Tiantian Geng, Huishan Lai, and Lei Jing. 2026. Enhancing VR Mandala Drawing and Natural Immersion for Attention Restoration with AI-Driven Bioadaptive Multimodal Interaction. In *The Augmented Humans International Conference 2026 (AHs 2026), March 16–19, 2026, Okinawa, Japan.* ACM, New York, NY, USA, 8 pages. https://doi.org/10.1145/3795011.3795053

1 Introduction

Continuous connectivity, fragmented workflows, and dense digital information loads make attention a scarce and fragile resource [1, 10]. Directed attention is limited and fatigue-prone; when repeatedly taxed, people require opportunities for restoration to maintain performance and well-being.

Attention Restoration Theory (ART) suggests that contact with natural environments can help restore directed attention [12, 13]. As everyday access to nature declines [24], virtual reality (VR) has been explored as a substitute, with nature-based VR shown to support attentional recovery [8, 17]. However, many restorative VR systems still emphasize passive viewing, leaving limited guidance on how interaction design should support attention regulation goals.

Attentional-ecology perspectives emphasize that restoration depends not only on exposure to nature, but on how tasks, environments, and internal states are coordinated over time [2, 25]. This motivates moving beyond passive exposure toward guided interaction. Structured activities such as mandala drawing have been used as *active centering* and linked to improved attention and reduced impulsivity [7, 25, 32]. Yet visuals alone may be insufficient for attention-related benefits [5], multisensory synchronization can strengthen immersion and performance [6, 22], but adding touch and smell did not significantly improve emotions or presence for VR relaxation induction [29]. These findings reveal a gap between theory and practice: designs must reconcile theoretical grounding with implementable interaction to ensure restorative benefits rather than added cognitive load.

Another related gap concerns personalization and in-process adaptation. Recent AI methods increasingly use electroencephalography (EEG) to recognize attention-related states and adapt VR content for attention and workload regulation [9, 18, 19, 36]. However, deploying EEG for robust real-time closed-loop VR remains

AHs 2026, Okinawa, Japan

ACM ISBN 979-8-4007-2351-3/26/03
https://doi.org/10.1145/3795011.3795053

difficult due to motion artifacts and limited online artifact suppression [14]. Heart-rate variability (HRV) and related autonomic signals can support real-time regulation of stress and attentional state [3, 23, 31]. Compared to EEG, HRV is typically easier to deploy for closed-loop control; however, practical guidance for *personalizing* physiology-to-feedback mappings remains limited, which can hinder individual-consistent restoration effects.

Finally, restorative VR outcomes should be evaluated with sufficient evidence. The Igroup Presence Questionnaire (IPQ) [27] characterizes experience, and the Perceived Restorativeness Scale (PRS) [11] captures perceived restorativeness. Some studies also consider objective proxies associated with relaxation and attention, such as EEG during VR nature exposure [4, 21], HRV as an autonomic marker linked to calm and attentional control [13, 28], and behavioral assessment via the visual oddball task [16]. However, evaluation in restorative VR often varies in measurement coverage and relies on a limited subset of measures, leaving conclusions supported by partial evidence.

Motivated by these gaps, this work explores how guided interaction in restorative VR can be linked to measurable restoration, and how deployable physiology can support individualized regulation during the experience. Our contributions are threefold:

- *Psychology-theory-guided experience design:* Grounded in ART and *attentional ecology*, we design and implement a restorative VR application that combines *virtual nature exposure* with a low-demand, structured *mandala activity*, as a theory-driven form of guided design for attention restoration.
- *Personalized bioadaptive interaction mechanism:* An AI-driven, HRV-centered adaptive loop was implemented to map individual physiological dynamics to multimodal interactive feedback, enabling personalized regulation during the experience.
- *Multidimensional evaluation:* An exploratory evaluation was reported across self-report, behavioral, autonomic, and electroencephalography outcomes, providing initial evidence and practical insights.

2 System and Implementation

2.1 System overview and instrumentation

Figure 1 shows the closed-loop architecture of our VR system. Users engage with the *Experience Intervention Layer* via a Meta Quest 2, which presents a static 360° nature scene (VR Nature Environment) and a mandala-coloring task (VR Drawing Module). During the session, ECG-derived R–R intervals from a Polar H10 are streamed to the PC-based *Bioadaptive Control Layer*, where HRV features are extracted to estimate arousal and generate policy-mapping control signals. The *Multimodal Rendering Layer* then applies these signals to modulate visual haze (fog), audio (music), and controller haptics, feeding back into the VR experience to complete the loop. For outcome assessment, we additionally record HRV (Polar H10) and EEG (Polymate Mini AP108) in pre/post evaluation blocks (Fig. 2).

2.2 VR Nature Scene and Mandala Drawing

The VR experience couples a static natural surround with low-demand, structured interaction (Fig. 3). The restorative context is a 360° panoramic seascape depicting a calm shoreline at sunset. The scene remains static to maintain low visual complexity and support ART-consistent qualities such as soft fascination, spatial extent, and a sense of being away [12]; it also aligns with commonly used notions of perceived restorativeness in restorative-environment research [11].

Within this natural backdrop, participants complete a mandala-coloring task using a symmetric template composed of stylized natural motifs (e.g., sun, birds, trees, mountains, and rivers). A floating palette supports color selection and erasing, and interaction is intentionally slow-paced to encourage mindful engagement and sustained attention without performance pressure.

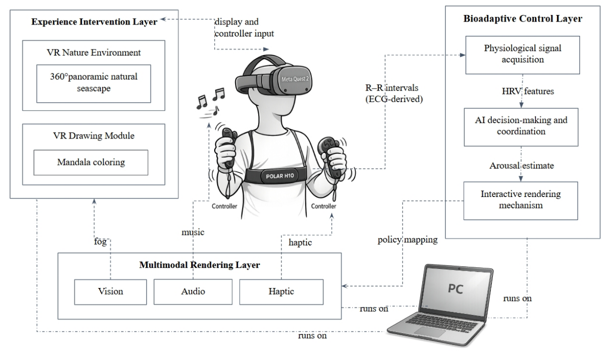

Figure 1: Overview of the system architecture.Users engage with a 360° nature scene and a mandala-coloring task in the *Experience Intervention Layer* (Meta Quest 2). ECG-derived R–R intervals from Polar H10 are processed on the PC to extract HRV features and estimate arousal, producing policy-mapping control signals. The *Multimodal Rendering Layer* applies these signals to visual haze (fog), audio (music), and controller haptics, completing the loop.

(a) Polar H10 ECG chest strap for HRV.

(b) Polymate Mini AP108 amplifier for EEG.

Figure 2: Instrumentation used in the study. (a) Polar H10 ECG chest strap providing R–R intervals for online closed-loop control and for pre/post HRV assessment . (b) Polymate Mini AP108 used for EEG acquisition in the pre/post blocks only.

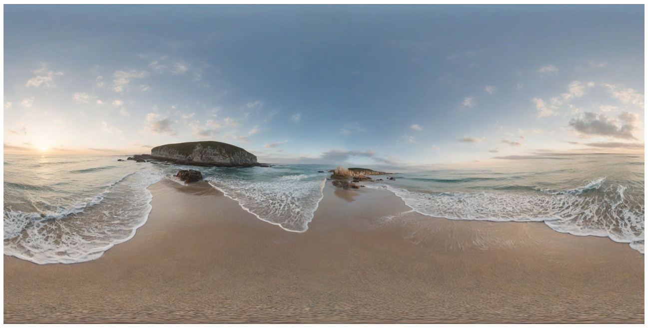

(a) Static 360° seascape used as the restorative background.

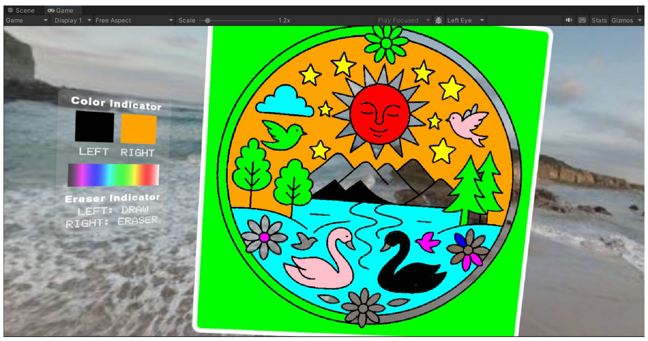

(b) VR mandala drawing interface.

Figure 3: VR nature scene and mandala drawing. VR mandala drawing task embedded in a static 360° natural seascape. The scene provides a low-arousal surround, while the mandala interface supports low-demand structured engagement.

2.3 AI-driven bioadaptive multimodal interaction

We implement an HRV-centered closed-loop module that maps autonomic dynamics to multimodal VR feedback while enabling lightweight personalization of feedback sensitivity. Beat-to-beat R–R intervals from a Polar H10 are streamed to a Python controller via Bluetooth Low Energy (BLE) and published through the Lab Streaming Layer (LSL). The controller buffers overlapping windows ($W = 45$ s, hop $\Delta = 1$ s) using cumulative physiological time and discards windows with fewer than 20 beats to avoid unstable ultra-short HRV estimates [20, 30]. For each valid window, timestamps are reconstructed, the tachogram is resampled (4 Hz) and detrended, and standard HRV indices are computed across time, frequency, and nonlinear domains using conventional bands [30, 33]. To reduce inter-individual offsets, features are normalized to an initial 1 min resting baseline by augmenting each feature with both $(x - \mu)$ and $(x - \mu)/\sigma$ (robust σ when needed).

Physiological state is estimated using an XGBoost classifier trained on WESAD [26] (stress vs. baseline+amusement; leave-one-subject-out AUROC = 0.92, $F_1 = 0.78$), yielding a continuous proxy $p_t \in [0, 1]$. To prevent control chattering, we stabilize p_t with an exponential moving average (EMA; $\alpha = 0.40$) and a dual-threshold hysteresis gate ($\tau_{\text{lo}} \approx 0.60 \cdot \text{THR}$, $\tau_{\text{hi}} \approx 0.85 \cdot \text{THR}$; THR is the F_1-optimal operating threshold), producing p_t^{ema} and a binary state $\hat{y}_t$ (Eq. 1).

Algorithm 1 Runtime loop for HRV-driven bioadaptive feedback with online gain selection

Input: Window length W, hop Δ; baseline normalizer; classifier $g(\cdot) \to p_t$.
Input: Gain presets C; ϵ-greedy bandit with hold time T_{hold}.
for each control tick (every Δ) **do**
  Sense: Extract HRV features $\mathbf{x}_t$ from the latest window and baseline-normalize.
  Estimate: $p_t \leftarrow g(\mathbf{x}_t)$; compute $(p_t^{\text{ema}}, \hat{y}_t)$ using Eq. 1.
  Adapt: Update bandit reward/utility from p_t^{ema} using Eq. 3; switch preset only if T_{hold} elapsed.
  Actuate: Map $(p_t^{\text{ema}}, \hat{y}_t)$ to fog/music with the active preset C_t (Eq. 2); send to Unity.
end for

The stabilized state drives a preset-based policy mapping from $(p_t^{\text{ema}}, \hat{y}_t)$ to multimodal feedback. Each gain preset $C_t \in C$ specifies channel gains and offsets for visual and audio feedback in Eq. 2. Specifically, the active preset modulates visual haze (fog-like clarity reduction via Universal Render Pipeline (URP) post-processing) and audio dynamics (mild tremolo and compression). To keep haptics synchronized with the delivered soundscape without adding a separate control stream, controller vibration is derived on the Unity client from the rendered audio via a windowed short-time Fourier transform (STFT; implemented with a fast Fourier transform, FFT) and scaled by the preset coupling gain. Control signals are smoothed and sent to Unity at 1 Hz.

To personalize feedback sensitivity, we address the gain-selection problem with an ϵ-greedy bandit over a small set of gain presets. The agent maintains a per-preset utility estimate updated from short-horizon changes in p_t^{ema} (Eq. 3) and selects the next preset under a minimum hold time T_{hold} (Alg. 1). End-to-end latency from R–R arrival at the LSL inlet to Unity parameter update was below 100 ms (mean 72 ± 14 ms).

$$p_t^{\text{ema}} = \alpha p_t + (1 - \alpha) p_{t-1}^{\text{ema}}, \qquad \hat{y}_t = \begin{cases} 1, & p_t^{\text{ema}} \geq \tau_{\text{hi}}, \\ 0, & p_t^{\text{ema}} \leq \tau_{\text{lo}}, \\ \hat{y}_{t-1}, & \text{otherwise.} \end{cases} \tag{1}$$

$$\begin{aligned} f_t &= \text{clip}\left(k_f^{(C_t)}\, p_t^{\text{ema}} + b_f^{(C_t)}\right), \\ m_t &= \text{clip}\left(k_m^{(C_t)}\, p_t^{\text{ema}} + b_m^{(C_t)}\right), \end{aligned} \tag{2}$$

$$r_t = \text{clip}\left(p_{\text{prev}} - p_{\text{now}},\ -0.5,\ 0.5\right). \tag{3}$$

3 Study Design

3.1 Research Hypotheses

(1) **H1 (within-condition restoration).** In both conditions, the VR experience was expected to show pre–post changes consistent with restoration: improved autonomic and electroencephalography markers, maintained or improved behavioral performance, and above-neutral self-report measures of presence and perceived restorativeness.

(2) **H2 (bioadaptive interaction advantage).** Compared to the no-multimodal-feedback condition, the AI-driven bioadaptive multimodal interaction condition was expected to yield higher self-report measures of presence and perceived restorativeness, and larger pre–post improvements in behavioral, autonomic, and electroencephalography measures.

3.2 Participants and Conditions

Eleven university students participated (N = 11, 6 male/5 female; age M = 25.9, SD = 2.3, range 23–31). The study was approved by the Research Ethics Committee of the University of Aizu (Approval No. 2025-Aizu-Kigyo-307), and all participants provided written informed consent.

We employed a within-subject, counterbalanced crossover design with two sessions on separate days (AI-first n = 6, NF-first n = 5). The two conditions were:

- **NF (No multimodal feedback):** VR mandala drawing within a static 360° seascape; no fog, music modulation, or controller haptics.
- **AI (AI-Driven bioadaptive multimodal interaction):** the same VR experience augmented with AI-driven bioadaptive feedback (visual fog, music modulation, and controller vibration).

3.3 Procedure

Before the experimental sessions, participants completed consent, a brief VR tutorial, and a demographic questionnaire. Participants then completed two experimental sessions (one per condition) on separate days.

Each session followed the same structure:

(1) **Oddball-pre (6 min).** Visual Oddball task with concurrent EEG and HRV, establishing baseline attentional and autonomic responses under cognitive demand.
(2) **VR intervention (10 min).** VR mandala drawing under AI or NF.
(3) **Oddball-post (6 min).** Repetition of the Oddball task with EEG and HRV.
(4) **Questionnaires (2–3 min).** Igroup Presence Questionnaire (IPQ, short form) [27] and an 8-item Perceived Restorativeness Scale (PRS) [11].

After both sessions, a short semi-structured interview collected qualitative impressions.

3.4 Measures

Self-report measures. IPQ short form (7-point Likert; scored 0–6) assessed Spatial Presence, Involvement, and General Presence [27], and score interpretation followed Tran et al. [34]. An 8-item PRS adapted from Hartig et al. [11] measured Being Away, Fascination, and Compatibility (0–6).

Behavioral measures. Behavioral performance was measured with a standard visual Oddball task [16]. Blue circles served as frequent standards and red circles as rare targets at fixation; participants responded only to targets. Each 6 min block comprised 160 trials (20% targets; 200 ms stimulus, 800 ms inter-stimulus interval). For each session and block (pre, post), we computed the median reaction time (RT) for correct targets and target-detection accuracy (hit rate). Change scores were defined as ΔRT = Pre − Post (positive = faster) and ΔAccuracy = Post − Pre.

Autonomic measures. R–R intervals were recorded continuously with a Polar H10 chest strap and analyzed in the Elite HRV application. We focused on three indices: lnRMSSD (vagal recovery), LF/HF ratio (sympathovagal balance) [33], and mean heart rate (bpm) as an index of overall cardiac activation [30].

EEG measures. EEG was recorded from Fz, Cz, Pz, Oz, and VEOG using the Polymate Mini AP108 system (500 Hz sampling) [35]. Signals were re-referenced to the average of scalp electrodes, bandpass filtered, and cleaned for motion and ocular artifacts. Relative band power in θ (Fz), α (Pz), and β (Cz) was estimated using Welch's method and interpreted as indices of cognitive control, attentional disengagement, and vigilance [15].

4 Results

All 11 participants completed both sessions and contributed usable data. HRV artifacts were rare (M = 0.29%), EEG segment retention was high (M = 88.0%), and condition order (AI–NF vs. NF–AI) did not significantly affect any change scores (all $p \geq .12$), so analyses use the full sample.

4.1 Self-report Questionnaires

Immersion (IPQ-6). Wilcoxon signed-rank tests (Table 1) suggested consistent trends favoring the AI condition, with the clearest gain in Spatial Presence ($Z = -1.84, p = .066, r = .61$) and a similar pattern for Overall IPQ ($Z = -1.69, p = .091, r = .51$); General Presence and Involvement were not statistically significant but showed medium-to-large effects (r = .28–.52). In terms of absolute levels, the 3D-HMD percentile-based ranking classes (Table 2) indicate a qualitative uplift: AI reached *Moderate* presence for Overall IPQ, Spatial Presence, and Involvement, whereas NF remained *Low* on these dimensions; General Presence increased numerically but stayed in the *Low* band.

Perceived restorativeness (PRS-8). PRS-8 ratings were generally at or above the neutral midpoint (3) in both conditions (Table 3), indicating that participants experienced the VR scene as restorative overall. Although none of the PRS comparisons reached statistical significance in this pilot sample, scores were consistently higher in AI than NF for Overall PRS and Fascination, with Fascination showing a medium effect size ($Z = -1.33, p = .180, r = .47$).

4.2 Behavioral Performance

Oddball performance remained high in both conditions (accuracy $\approx$ .99), with only small pre–post changes in reaction time. RT slowed slightly after the VR break in both NF and AI, and the between-condition difference was negligible (AI vs. NF: $\Delta\Delta M \approx -2$ ms, p = .835). Thus, enabling AI-driven bioadaptive feedback did not introduce any measurable cost to task performance.

4.3 Autonomic Physiology

HRV patterns indicated mild autonomic recovery in both conditions. Mean heart rate decreased slightly in NF and AI (both by

Table 1: IPQ Wilcoxon signed-rank Results (Median [IQR], NF vs. AI).

Measure	Median (NF) [Q1, Q3]	Median (AI) [Q1, Q3]	$n^\dagger$	Z	p	$r^\ddagger$
Overall IPQ	3.50 [2.08, 4.00]	4.50 [2.58, 4.83]	11	−1.69	.091§	.51
General Presence (G1)	4.00 [1.50, 5.00]	4.00 [3.00, 5.00]	8	−0.78	.435	.28
Spatial Presence (SP)	3.67 [2.00, 4.17]	4.33 [3.33, 5.50]	9	−1.84	.066§	.61
Involvement (INV)	3.00 [2.00, 3.00]	4.00 [1.75, 4.75]	8	−1.47	.141	.52

Note. Scores range from 0 to 6. Two-sided Wilcoxon signed-rank tests were performed. The item "I still paid attention to the real environment" was reverse-coded prior to computing INV and Overall IPQ aggregates. $^\dagger n$ is the number of non-zero paired differences (zero-difference pairs are omitted). ‡ Effect size is computed as $r = |Z|/\sqrt{n}$ (small $\geq$ .10, medium $\geq$ .30, large $\geq$ .50). § $p < .10$.

Table 2: IPQ Level (Mean±SD, NF vs. AI).

Condition	Overall (M±SD)	Class	GP (M±SD)	Class	SP (M±SD)	Class	INV (M±SD)	Class
NF	3.00 ± 1.40	Low	3.18 ± 1.89	Low	3.06 ± 1.68	Low	2.82 ± 1.37	Low
AI	3.74 ± 1.56	Moderate	3.64 ± 1.63	Low	3.97 ± 1.86	Moderate	3.45 ± 1.75	Moderate

Note. Ranking classes follow the percentile schema (Low < P50; Moderate ≥ P50; High ≥ P75; Very High ≥ P90; Exceptional ≥ P95). Thresholds were defined on the original IPQ scale [-3, 3] and shifted by +3 to match our 0–6 scoring. For the **Overall** score: P50=3.34, P75=3.80, P90=4.16, P95=4.32; for **GP**: P50=4.00, P75=4.50, P90=4.91, P95=5.10; for **SP**: P50=3.72, P75=4.30, P90=4.74, P95=4.99; for **INV**: P50=3.26, P75=3.76, P90=4.06, P95=4.28.

Table 3: PRS Wilcoxon signed-rank Results (Median [IQR], NF vs. AI).

Measure	Median (NF) [Q1, Q3]	Median (AI) [Q1, Q3]	$n^\dagger$	Z	p	$r^\ddagger$
Overall PRS	3.75 [1.56, 4.69]	4.00 [2.94, 4.44]	10	−1.02	.307	.32
Being Away	3.00 [1.00, 5.00]	3.33 [2.00, 4.67]	8	−0.28	.779	.10
Fascination	3.50 [1.75, 4.50]	4.00 [3.25, 4.75]	8	−1.33	.180	.47
Compatibility	4.00 [2.33, 5.00]	4.00 [3.33, 4.33]	8	−0.49	.622	.17

Note. Scores range from 0 to 6; values above 3 indicate above-neutral perceived restorativeness. Two-sided Wilcoxon signed-rank tests were performed. $^\dagger n$ is the number of non-zero paired differences (zero-difference pairs are omitted). ‡ Effect size is computed as $r = |Z|/\sqrt{n}$ (small $\geq$ .10, medium $\geq$ .30, large $\geq$ .50).

$\approx$ 0.7–0.8 bpm), and lnRMSSD (vagal activity) increased only in NF (from 4.10 to 4.24; $\Delta M = 0.14$, $d_z \approx 0.6$), but not in AI (4.13 to 4.12). The LF/HF ratio decreased in both conditions (NF: 1.73 to 1.49; AI: 1.88 to 1.38), with a numerically larger drop in AI (about −0.5 vs. −0.2 in NF), yet difference-in-differences effects were small and non-significant across all three indices (all $p > .20$, $|d_z| < 0.45$). Taken together, this pattern suggests *complementary regulatory mechanisms*: NF primarily supports vagal upregulation, whereas enabling bioadaptive feedback tends to promote a stronger rebalancing of sympathovagal activity without changing overall heart rate.

4.4 EEG Outcomes

Figure 4 summarizes relative power changes in Pz α, Fz θ, and Cz β. Given the pilot sample size ($N = 11$), we analyzed between-condition differences in paired pre–post change scores (Δ = Post − Pre) using two-sided Wilcoxon signed-rank tests on paired within-subject differences, testing whether $d_i = \Delta_{i,\mathrm{AI}} - \Delta_{i,\mathrm{NF}}$ differs from zero. We report the Wilcoxon statistic (W), two-sided p values, and rank-biserial correlations (r_{rb}) as effect sizes.

Alpha / Theta trends (H1). Pz α showed a numerically larger increase under AI ($Mdn_\Delta = +0.0146$) than NF ($Mdn_\Delta = +0.0024$). However, the between-condition difference in change scores was not statistically significant ($W = 16$, $p = .147$, $r_{rb} = 0.52$; Fig. 4B, middle). Fz θ change scores did not differ reliably between conditions ($W = 32$, $p = .966$, $r_{rb} = -0.03$; Fig. 4B, left).

Beta arousal regulation (H2). Cz β exhibited a clear divergence between conditions, yielding a **significant between-condition difference** with a large effect size ($W = 9$, $p = .032$, $r_{rb} = -0.73$; Fig. 4B, right). Whereas NF showed a positive post–pre change ($Mdn_\Delta = +0.0135$), AI showed a negative change ($Mdn_\Delta = -0.0086$). Together, these results indicate that the AI condition was associated with a lower post–pre β change than the NF condition in this pilot sample.

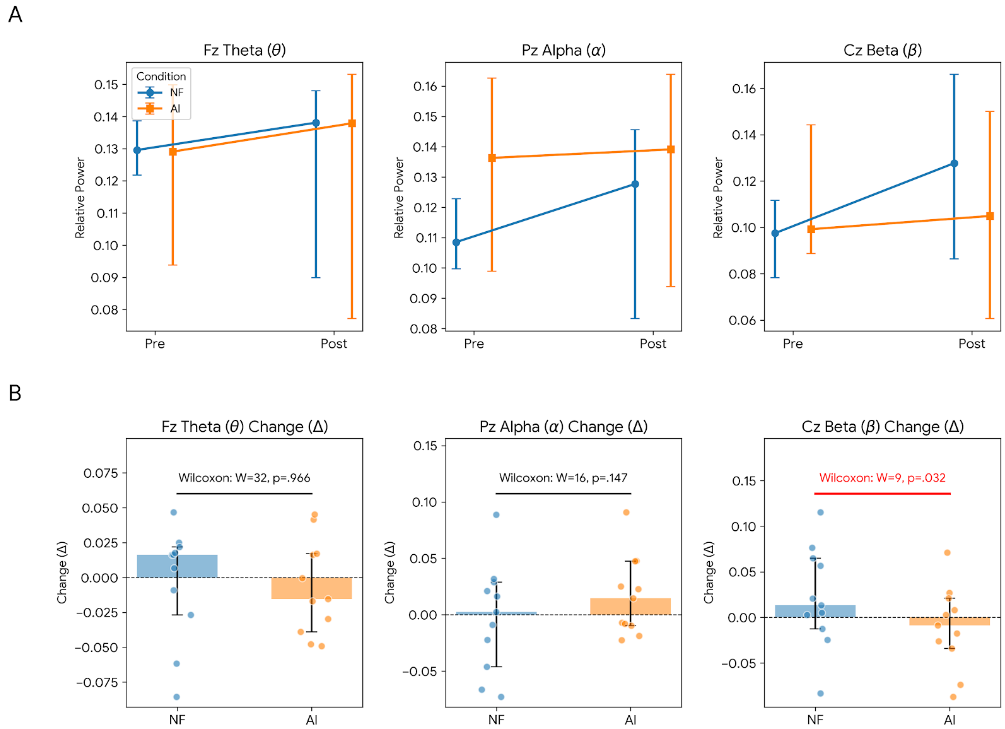

Figure 4: EEG results. Top (A): Pre/post relative power for Fz θ, Pz α, and Cz β. Markers indicate sample medians; error bars indicate the interquartile range (IQR; 25th–75th percentiles). Bottom (B): Paired change scores (Δ = Post − Pre). Bars indicate the median Δ; error bars indicate nonparametric 95% bootstrap confidence intervals for the median (percentile, 10,000 resamples). Dots show individual participants' Δ values. Between-condition differences were assessed using two-sided paired Wilcoxon signed-rank tests on $d_i = \Delta_{i,\mathrm{AI}} - \Delta_{i,\mathrm{NF}}$ (reported as W and p). Cz β shows a significant divergence ($W = 9$, $p = .032$): AI shows a negative Δ while NF shows a positive Δ.

Table 4: Qualitative themes and representative quotes.

Theme	Representative quote(s)
Restorative experience	*"I like drawing in the VR world, it makes me relax."*
Usability & fatigue	*"It was fun to color with just one click."* *"The first session was too tiring… because of VR hand position."*
Future expectations	*"Surrounding will be a dynamic, not static picture."* *"Maybe add more pictures and more colors to choose."*

4.5 Qualitative Feedback

To contextualize the questionnaire results, we performed a lightweight thematic analysis of post-study semi-structured interviews and open-ended responses. Three recurring themes emerged (Table 4).

Overall, participants frequently described the experience as calming and comfortable, consistent with above-neutral PRS scores. The "one-press" coloring interaction was commonly described as easy to use, while some participants reported arm/hand fatigue or occasional tracking issues during prolonged gestures. Participants also expressed interest in more dynamic and customizable content (e.g., moving elements and selectable scenes), suggesting opportunities to improve engagement in future iterations.

4.6 Condition-stratified fascination–recovery coupling

Condition-stratified (within-condition) associations between perceived restorativeness and behavioral recovery were examined. Oddball RT improvement was defined as $RT_{\mathrm{Pre}} - RT_{\mathrm{Post}}$ (positive values indicate faster post-intervention responses). In the NF condition, PRS Fascination was not reliably related to RT improvement (Spearman $\rho_s = -0.31$, $p = .362$). In contrast, under bioadaptive interaction (AI), higher Fascination was associated with greater RT improvement (Spearman $\rho_s = 0.76$, $p = .007$; Fig. 5). This condition-specific coupling suggests that AI-driven bioadaptive multimodal interaction may strengthen the link between perceived restorativeness and measurable attentional recovery.

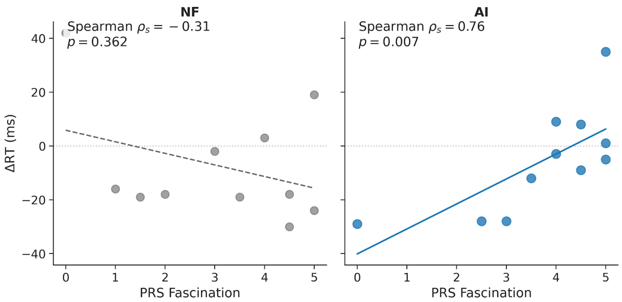

Figure 5: Condition-specific fascination–recovery coupling ($N = 11$). PRS Fascination vs. Oddball RT improvement within NF and AI. RT improvement: $RT_{\text{Pre}} - RT_{\text{Post}}$ (positive = faster). Spearman: NF $\rho_s = -0.31$ ($p = .362$), AI $\rho_s = 0.76$ ($p = .007$).

5 Discussion

This study examined whether adding AI-driven bioadaptive multimodal interaction to a VR nature-and-mandala experience shapes attention restoration relative to a no-multimodal-feedback baseline. The pattern across measures suggests two complementary points: (i) both conditions can support restorative *experience* (self-report; Tables 1–3), and (ii) bioadaptive interaction can shift *regulation* signatures that are less visible in self-report alone (electroencephalography; Fig. 4). An additional implication is that bioadaptive interaction may strengthen the behavioral relevance of perceived restorativeness (Fig. 5).

5.1 Experience-level restoration across conditions

Above-neutral PRS and meaningful presence in both conditions indicate that the combination of a calm natural surround and a low-demand structured activity is sufficient to yield restorative experiences for many users (Tables 1–3). However, electroencephalography results show that comparable subjective restoration does not necessarily imply comparable regulation dynamics: the Cz β divergence (Fig. 4) suggests that physiology-driven multisensory modulation can alter post-intervention arousal regulation even when self-report differences are modest. This supports the view that restorative XR should be evaluated not only by how restorative it *feels*, but also by how regulation markers shift following the intervention.

5.2 Autonomic and behavioral sensitivity under a short-dose protocol

The lack of clear between-condition differences in autonomic indices and mean reaction time should be interpreted in the context of measurement sensitivity under a short-dose protocol. Behavioral headroom was limited by near-ceiling Oddball accuracy and small RT changes, which reduces the ability to detect incremental benefits. Autonomic responses also exhibited visible inter-individual variability, and qualitative feedback points to potential ergonomic load (arm/hand fatigue, occasional tracking issues; Table 4) that could partially mask relaxation-related physiology. Together, these factors suggest that longer or repeated sessions, extended post-intervention recovery windows, and improved ergonomics may be necessary before autonomic and behavioral effects can reliably emerge.

5.3 Experience–recovery coupling under bioadaptation

The condition-specific Fascination–RT association (Fig. 5) provides a hypothesis-generating mechanistic clue: perceived fascination appears more behaviorally informative when multisensory feedback is coupled to autonomic state. One interpretation is that bioadaptive modulation helps stabilize engagement at a restorative "sweet spot," improving alignment between subjective experience and attentional recovery outcomes. Notably, this coupling does not imply that stronger subjective restoration always yields larger physiological changes; rather, it suggests that bioadaptation can reshape how experience relates to function, which may be valuable for designing interventions that aim to translate relaxation into performance-relevant recovery.

5.4 Limitations and future work

This pilot study is limited by sample size and exploratory analyses. Future work should validate these patterns with larger samples, longer or repeated-use protocols, and factorial designs that separate the effects of multimodal stimulation from closed-loop bioadaptive control. Incorporating more sensitive behavioral probes and reducing mid-air interaction load may further clarify when and for whom bioadaptive multimodal interaction yields measurable benefits.

6 Conclusion

This work introduced a *psychology-theory-guided* and deployable bioadaptive VR intervention for digital attention fatigue. Grounded in Attention Restoration Theory and an attentional-ecology perspective, the system couples a low-demand, structured mandala activity with a static 360° natural scene and uses heart rate variability to drive an AI-based, personalized multimodal feedback loop (visual haze, adaptive audio, and synchronized haptics) with online gain personalization.

Across a within-subject pilot study ($N = 11$), both the *no-multimodal-feedback condition* and the *AI-driven bioadaptive multimodal interaction condition* were experienced as generally restorative (above-neutral perceived restorativeness and meaningful presence). Beyond these shared positive experiences, bioadaptive multimodal interaction yielded a distinct regulatory signature: a significantly lower post–pre change in arousal-related Cz β power relative to the no-multimodal-feedback condition, consistent with altered electroencephalography-based arousal regulation following the intervention. In addition, a condition-specific coupling emerged in which PRS Fascination covaried with reaction-time improvement only when bioadaptive multimodal interaction was enabled, suggesting that perceived restorativeness may become more behaviorally informative under physiology-driven adaptation.

Taken together, the findings support three contributions: (i) a psychology-theory-guided experience design that operationalizes restorative principles through a structured, low-demand activity embedded in a calm natural surround; (ii) a personalized bioadaptive interaction mechanism that maps real-time autonomic dynamics to multimodal feedback with deployable sensing and lightweight online personalization; and (iii) evidence for the value of *multidimensional evaluation*, where self-report measures alone indicated broadly positive experiences while behavioral, autonomic, and electroencephalography measures revealed limited behavioral headroom, heterogeneous autonomic responses, and a clear neural divergence under bioadaptation. Future work should test longer and repeated-use protocols, improve interaction ergonomics, and adopt factorial designs that disentangle multimodal stimulation from bioadaptive control while validating generalization across populations and settings.

Acknowledgments

This work was supported by NEDO Intensive Support for Young Promising Researchers Number 21502121-0, Collaborative Research with Toyota Motor Corporation, and JKA and its promotion funds from KEIRIN RACE.

References

[1] Asma Asfour. 2024. *Capturing Minds: Understanding the Attention Economy.* Self-published.

[2] Adam C. Barton, Jade Sheen, and Linda K. Byrne. 2020. Immediate attention enhancement and restoration from interactive and immersive technologies: A scoping review. *Frontiers in Psychology* 11 (2020), 2050. doi:10.3389/fpsyg.2020.02050

[3] Johannes Blum, Christoph Rockstroh, and Anja S. Göritz. 2019. Heart rate variability biofeedback based on slow-paced breathing with immersive virtual reality nature scenery. *Frontiers in Psychology* 10 (2019), 2172. doi:10.3389/fpsyg.2019.02172

[4] Jiayin Chen, Huiqiu Zhu, Yue Cheng, Henan Yin, Minzhe Yi, Danni Shen, Zuyao Zhang, and Jue Wu. 2025. Restorative effects and perception of nature-themed artworks in indoor environments: An empirical study based on VR and EEG. *Frontiers in Psychology* 16 (2025), 1571176. doi:10.3389/fpsyg.2025.1571176

[5] Sara A Collins, Amy S McDonnell, Emily E Scott, Glen D McNay, Mary F Shannon, Lensky Augustin, Janet Nicole Hoffmann, Sharde Johnson, David L Strayer, and Sara B LoTemplio. 2025. Nature imagery's influence on ERN amplitude: an examination of Attention Restoration Theory using EEG. *Frontiers in Human Neuroscience* 19 (2025), 1567689.

[6] Natalia Cooper, Ferdinando Milella, Carlo Pinto, Iain Cant, Mark White, and Georg Meyer. 2018. The effects of substitute multisensory feedback on task performance and the sense of presence in a virtual reality environment. *PLOS ONE* 13, 2 (2018), e0191846.

[7] Nancy A Curry and Tim Kasser. 2005. Can coloring mandalas reduce anxiety? *Art Therapy* 22, 2 (2005), 81–85.

[8] Nikolaos Drakatos, Nikolaos Bardis, Charalabos Skianis, and Athanasios Drigas. 2025. Effectiveness of virtual reality in attention. *Frontiers in Human Neuroscience* (2025).

[9] Alessandro Frolli, Emilio Saviano, Mariacarla Ricci, Simona Luigia Sica, and Marco Romano. 2024. Artificial Intelligence in ADHD Treatment: A Brief Narrative Review. *Digital Innovations for Learning and Neurodevelopmental Disorders* 3751 (2024).

[10] Adam Gazzaley and Larry D. Rosen. 2016. *The Distracted Mind: Ancient Brains in a High-Tech World.* MIT Press.

[11] Terry Hartig, Kalevi Korpela, Gary W. Evans, and Tommy Gärling. 1997. A Measure of Restorative Quality in Environments. *Scandinavian Housing and Planning Research* 14, 4 (1997), 175–194. doi:10.1080/02815739708730435

[12] Rachel Kaplan and Stephen Kaplan. 1989. *The Experience of Nature: A Psychological Perspective.* Cambridge University Press.

[13] Stephen Kaplan. 1995. The restorative benefits of nature: Toward an integrative framework. *Journal of Environmental Psychology* 15, 3 (1995), 169–182.

[14] Atilla Kilicarslan and José Luis Contreras-Vidal. 2017. Full characterization and removal of motion artifacts from scalp EEG recordings. In *Proceedings of the 2017 International Symposium on Wearable Robotics and Rehabilitation (WeRob).* IEEE, 1. doi:10.1109/WeRob.2017.8467841

[15] René Labounek, Martin Lamoš, Radek Mareček, Milan Brázdil, and Jiří Jan. 2015. Exploring Task-Related Variability in fMRI Data Using Fluctuations in Power Spectrum of Simultaneously Acquired EEG. *Journal of Neuroscience Methods* 245 (2015), 125–136. doi:10.1016/j.jneumeth.2015.02.016

[16] Fali Li, Chanlin Yi, Yuanling Jiang, Yuanyuan Liao, Yajing Si, Jing Dai, Dezhong Yao, Yangsong Zhang, and Peng Xu. 2019. Different contexts in the oddball paradigm induce distinct brain networks in generating the P300. *Frontiers in Human Neuroscience* 12 (2019), 520.

[17] Gang Li, Joaquin A. Anguera, Samirah V. Javed, Muhammad Adeel Khan, Guoxing Wang, and Adam Gazzaley. 2020. Enhanced attention using head-mounted virtual reality. *Journal of Cognitive Neuroscience* 32, 8 (2020), 1438–1454. doi:10.1162/jocn_a_01552

[18] Gang Li and Muhammad Adeel Khan. 2019. Deep learning on VR-induced attention. In *Proceedings of the 2019 IEEE International Conference on Artificial Intelligence and Virtual Reality (AIVR).* IEEE, 163–173. doi:10.1109/AIVR46125.2019.00033

[19] Gang Li, Shihong Zhou, Zhen Kong, and Mengyuan Guo. 2020. Closed-loop attention restoration theory for virtual reality-based attentional engagement enhancement. *Sensors* 20, 8 (2020), 2208.

[20] Kai Li, Heinz Rüdiger, and Tjalf Ziemssen. 2019. Spectral analysis of heart rate variability: time window matters. *Frontiers in neurology* 10 (2019), 545.

[21] Elisa Magosso, Francesca De Crescenzio, Giulia Ricci, Sergio Piastra, and Mauro Ursino. 2019. EEG alpha power is modulated by attentional changes during cognitive tasks and virtual reality immersion. *Computational Intelligence and Neuroscience* 2019 (2019), 7051079. doi:10.1155/2019/7051079

[22] Daniel Martin, Sandra Malpica, Diego Gutierrez, Belen Masia, and Ana Serrano. 2022. Multimodality in VR: A Survey. *Comput. Surveys* 54, 10s (2022), 1–36.

[23] Rollin McCraty and Fred Shaffer. 2015. Heart rate variability: New perspectives on physiological mechanisms, assessment of self-regulatory capacity, and health risk. *Global Advances in Health and Medicine* 4, 1 (2015), 46–61. doi:10.7453/gahmj.2014.073

[24] David G. Pearson and Tony Craig. 2014. The Great Outdoors? Exploring the Mental Health Benefits of Natural Environments. *Frontiers in Psychology* 5 (2014), 963. doi:10.3389/fpsyg.2014.00963

[25] Teresa P. Pham and Thomas Sanocki. 2024. Human Attention Restoration, Flow, and Creativity: A Conceptual Integration. *Journal of Imaging* 10, 4 (2024), 83. doi:10.3390/jimaging10040083

[26] Philip Schmidt, Attila Reiss, Robert Duerichen, Claus Marberger, and Kristof Van Laerhoven. 2018. Introducing WESAD, a Multimodal Dataset for Wearable Stress and Affect Detection. In *Proceedings of the 20th ACM International Conference on Multimodal Interaction (ICMI '18).* ACM, New York, NY, USA, 400–408. doi:10.1145/3242969.3242985

[27] Thomas Schubert, Frank Friedmann, and Holger Regenbrecht. 2001. The Experience of Presence: Factor Analytic Insights. *Presence: Teleoperators and Virtual Environments* 10, 3 (2001), 266–281. doi:10.1162/105474601300343603

[28] Emily E. Scott, Amy S. McDonnell, Sara B. LoTemplio, Bert N. Uchino, and David L. Strayer. 2021. Toward a Unified Model of Stress Recovery and Cognitive Restoration in Nature. In *Parks Stewardship Forum*, Vol. 37. JSTOR, 46–60.

[29] Berenice Serrano, Rosa M Baños, and Cristina Botella. 2016. Virtual reality and stimulation of touch and smell for inducing relaxation: A randomized controlled trial. *Computers in Human Behavior* 55 (2016), 1–8.

[30] Fred Shaffer and Jay P. Ginsberg. 2017. An Overview of Heart Rate Variability Metrics and Norms. *Frontiers in Public Health* 5 (2017), 258. doi:10.3389/fpubh.2017.00258

[31] Agnieszka Siennicka, Daniel S. Quintana, Piotr Fedurek, Agata Wijata, Beata Paleczny, Beata Ponikowska, and Dariusz Danel. 2019. Resting heart rate variability, attention and attention maintenance in young adults. *International Journal of Psychophysiology* 143 (2019), 126–131. doi:10.1016/j.ijpsycho.2019.06.017

[32] Valerie Smitheman-Brown and Robin R. Church. 1996. Mandala drawing: Facilitating creative growth in children with ADD or ADHD. *Art Therapy* 13, 4 (1996), 252–260. doi:10.1080/07421656.1996.10759233

[33] Task Force of the European Society of Cardiology and the North American Society of Pacing and Electrophysiology. 1996. Heart Rate Variability: Standards of Measurement, Physiological Interpretation and Clinical Use. *Circulation* 93, 5 (1996), 1043–1065. doi:10.1161/01.CIR.93.5.1043

[34] Tanh Quang Tran, Tobias Langlotz, Jacob Young, Thomas W. Schubert, and Holger Regenbrecht. 2024. Classifying Presence Scores: Insights and Analysis from Two Decades of the Igroup Presence Questionnaire (IPQ). *ACM Transactions on Computer-Human Interaction* 31, 5 (2024), 1–26. doi:10.1145/3689046

[35] Yusuke Yokota, Shingo Tanaka, Akihiro Miyamoto, and Yasushi Naruse. 2017. Estimation of Human Workload from the Auditory Steady-State Response Recorded via a Wearable Electroencephalography System during Walking. *Frontiers in Human Neuroscience* 11 (2017), 314. doi:10.3389/fnhum.2017.00314

[36] Teddy Marcus Zakaria, Armein Z. R. Langi, N. Muhamad Sophian, and Isa Anshori. 2025. Artificial Intelligence (AI) in Neurofeedback Therapy Using Electroencephalography (EEG), Heart Rate Variability (HRV), and Galvanic Skin Response (GSR). *IEEE Access* (2025). doi:10.1109/ACCESS.2025.3582805